Journal of Electrostatics 67 (2009) 123–127

Contents lists available at ScienceDirect

Journal of Electrostatics

journal homepage: www.elsevier.com/locate/elstat

Electrohydrodynamic flow patterns in a narrow electrostatic precipitator with longitudinal or transverse wire electrode

A. Niewulis [a,*], J. Podliński [a], J. Mizeraczyk [a,b]

[a] Centre for Plasma and Laser Engineering, The Szewalski Institute of Fluid Flow Machinery, Polish Academy of Sciences, Fiszera 14, 80-952 Gdańsk, Poland
[b] Department of Marine Electronics, Gdynia Maritime University, Morska 81-87, 81-225 Gdynia, Poland

ARTICLE INFO

Article history:
Received 24 September 2008
Received in revised form
19 November 2008
Accepted 6 January 2009
Available online 24 January 2009

Keywords:
Electrostatic precipitator
Narrow ESP
EHD flow
PIV measurements

ABSTRACT

Results of 2- and 3-dimensional Particle Image Velocimetry (PIV) measurements of the flow velocity fields in narrow electrostatic precipitators (ESPs) with either a longitudinal or transverse wire electrode are presented in this work. The obtained results confirmed that the particle flow in the ESP have a strongly 3D character mainly due to applied voltage and narrow cross section of the ESP duct. It was found that several vortices were formed along and across the ESP duct. The complex character of the flow in both ESP may considerably affect the particle collection efficiency of the ESP. This issue is under investigation.

1. Introduction

The electrostatic precipitators (ESPs) in spite of high overall collection efficiency (about 99.5%) are not efficient for reduction of submicron particles [1,2]. The fine particle collection efficiency in typical ESPs is low, typically of 70–80%. The collecting of fine particles is very important, because many of them, having a size from 0.1 μm to 1 μm have a detrimental effect on human and animal health. The fine particles may contain hazardous trace elements such as lead, mercury, arsenic, zinc, biological agents and others.

The collection efficiency of ESP is strongly dependent on the dust-particle properties, electric field, space charge, particle physical parameters and electrode geometry. The interaction between the electric field, space charge and gas flow results in considerable turbulence of the flow [3–10], which seems to lower the fine particle collection efficiency. According to [8–10], the turbulence should be reduced to improve the fine particle collection efficiency. Also improving other factors, such as ESP electrode geometry or ESP operating conditions may also increase the fine particle collection efficiency. Therefore, knowledge of the flow patterns in ESPs is essential for studying the performance of ESPs.

In this paper results of 2- and 3-dimensional Particle Image Velocimetry (PIV) measurements of the flow velocity fields in narrow ESPs with either a longitudinal or *transverse* wire electrode are presented.

2. Experimental apparatus

The experimental apparatus used in the present work consisted of an ESP, high voltage supply and standard 2D or 3D PIV equipment [11] for the measurement of velocity field (Fig. 1).

The ESP with longitudinally to flow placed wire electrode was a parallelepiped (300 mm × 30 mm × 30 mm) made of a glass and the ESP with transversely to flow placed wire electrode was made of a transparent acrylic (900 mm × 40 mm × 50 mm) (Fig. 2). The collecting electrodes were two plates placed along the ESP at its bottom and top. For ESP with longitudinal wire electrode two versions of ESP were used: A and B (Fig. 2a and b). In version B plate electrodes were 120 mm long. Similarly, for ESP with transverse wire electrode versions C and D were used (Fig. 2c and d). In version D plate electrodes were 180 mm long.

The positive voltage of up to 18 kV was applied to the wire electrode through a 10 MΩ resistor, while the collecting electrodes were grounded. The experiment was carried out with cigarette smoke as a tracer particles (particles size less than 1 μm in dry air). Air flow seeded with a cigarette smoke was blown along the ESP duct with an average velocity of up to 0.9 m/s. The PIV

* Corresponding author.
E-mail address: aniewulis@imp.gda.pl (A. Niewulis).

0304-3886/$ – see front matter © 2009 Published by Elsevier B.V.
doi:10.1016/j.elstat.2009.01.001

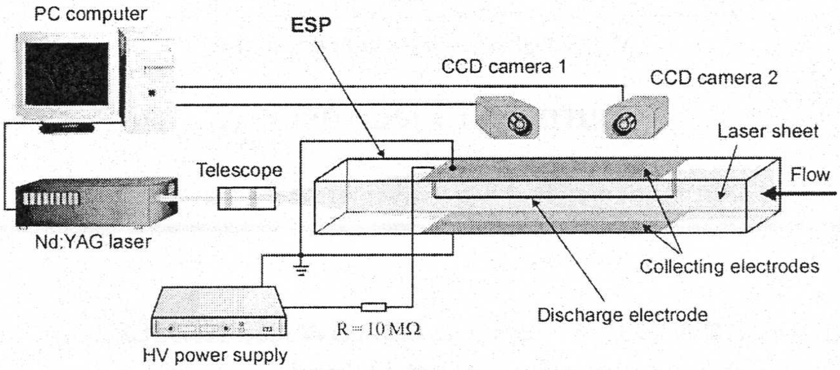

Fig. 1. Experimental set-up for 3D PIV measurement in the ESP with longitudinal wire electrode.

measurements were carried out in several planes along and across the ESP duct (see Fig. 2).

All the velocity fields presented in this paper resulted from the averaging of 100 measurements. Based on the measured velocity fields, the flow streamlines of a 2D flow were calculated.

3. Results

3.1. The ESP with longitudinal wire electrode

The 3D longitudinal particle flow patterns (i.e. measured in the measurement planes along the ESP) for the ESP with longitudinal wire electrode are shown in Fig. 3a–f. They show the velocity fields and the corresponding flow streamlines in the x–y plane as well as the z-component of the flow velocity.

The particle flow velocity fields measured by PIV method reflect of the dust particles in the ESP. When no voltage is applied, the submicron dust particles followed the gas main flow and, in this case, the measured velocity field of the particles corresponds to the gas flow velocity field. The particle flow velocity fields (and the corresponding flow streamlines) in Fig. 3 differ slightly from the gas flow velocity fields (and the corresponding flow streamlines). To obtain the gas flow patterns one has to subtract the particle drift velocity from the measured particle velocity. However, this requires a complex computing of the drift of the charged particles in the electric field with a space charge in the flowing gas. However, the drift velocity of fine particles of a few cm/s is considerably smaller than the gas velocity in the whole ESP duct, except in the area around the wire where the electric field is very high. This means that the

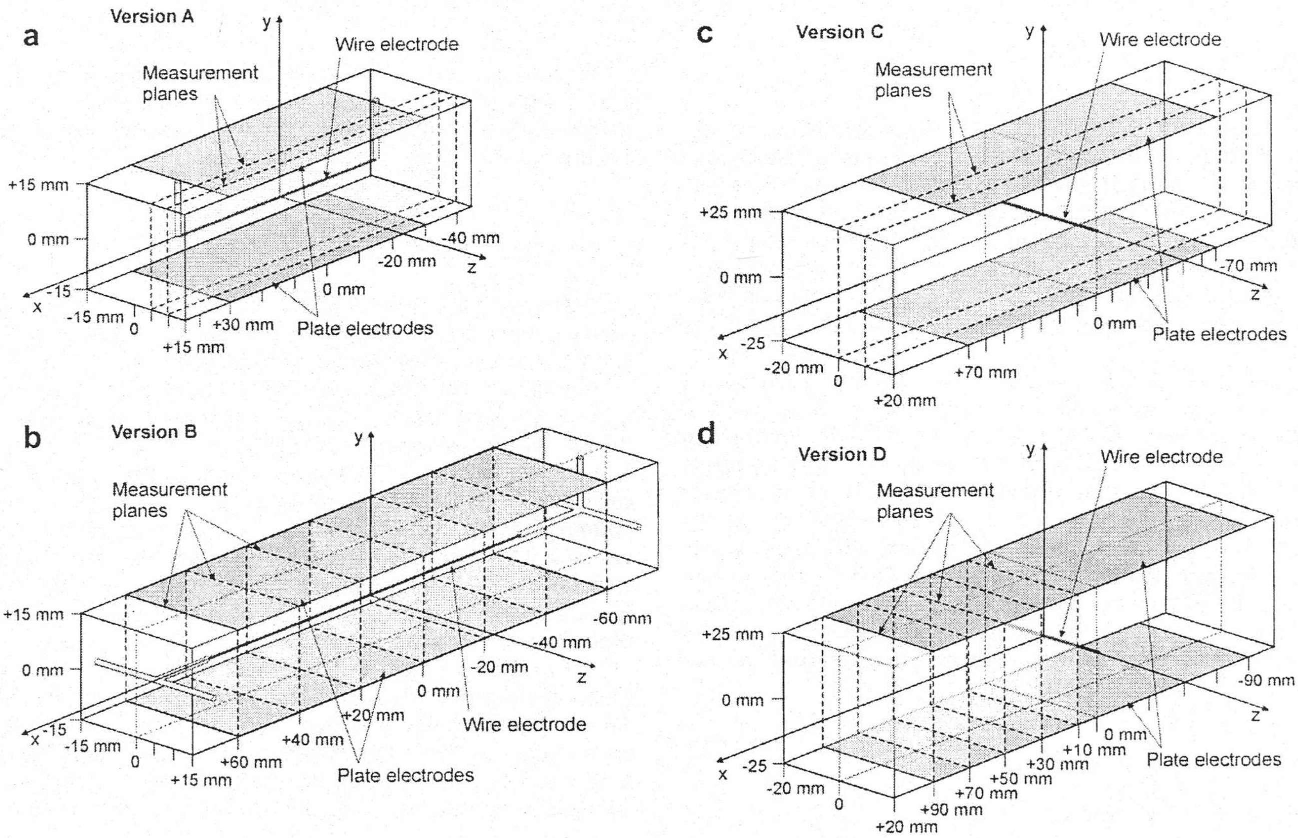

Fig. 2. The ESPs with longitudinal wire electrode (a, b) or with transverse wire electrode (c, d) with marked observation planes.

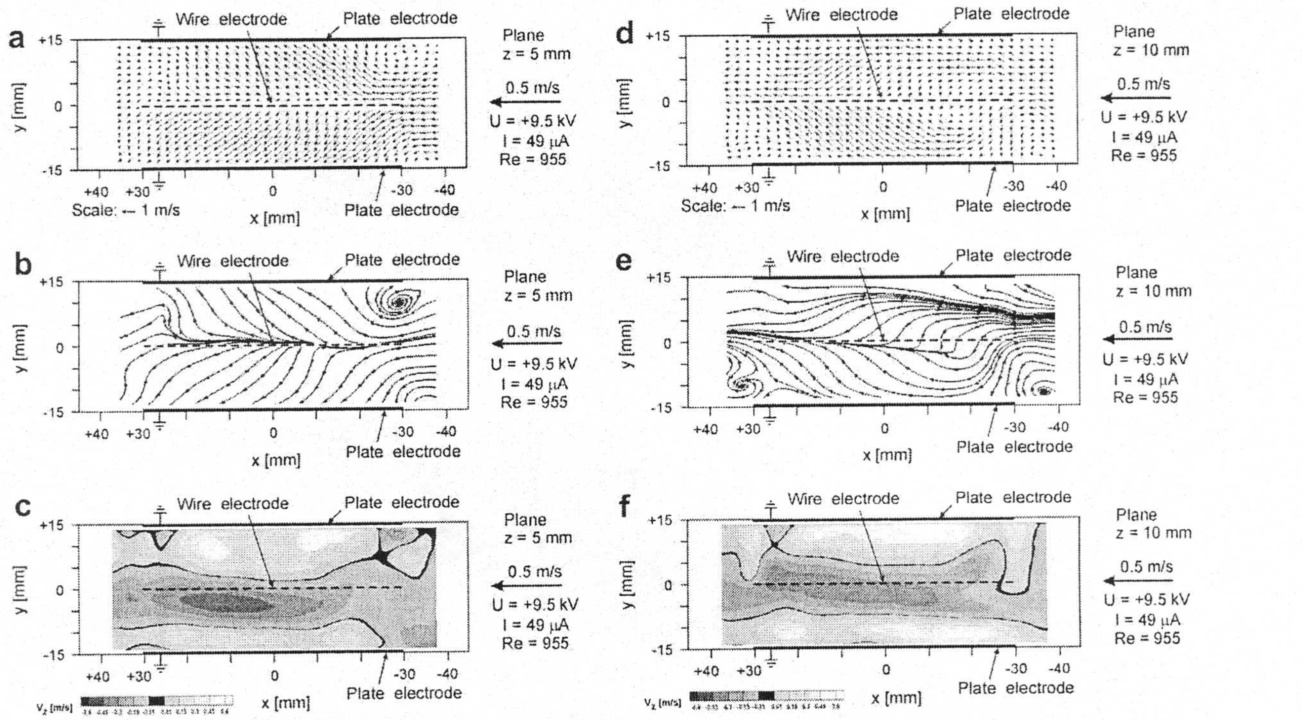

Fig. 3. Results of 3D PIV measurement in the ESP with longitudinal wire electrode in the plane at $z = +5$ mm and at $z = +10$ mm. The flow velocity field (a, d), the corresponding flow streamlines (b, e), and the velocity z-component (c, f).

gas flow patterns in the ESP can be reasonably well represented by the particle flow patterns presented in Fig. 3.

Fig. 3a–c shows the longitudinal particle flow patterns in the measurement plane at $z = +5$ mm. It is seen from Fig. 3a and b, that the particle flow pattern in the x–y plane is affected by the applied electric field not only in the discharge region and downstream but also before the discharge region, which begins at $x = -30$ mm. From this point on the particle trajectories are strongly bent towards the plate electrodes. Around $x = -30$ mm a vortex is formed. However, the most pronounced deflection of the particles towards the plate electrodes occurs between $x = -15$ mm and $x = +15$ mm of the discharge region. The particle movement in the z-direction is presented in Fig. 3c. It is seen that the particles being near the duct axis are moved towards the wire electrode, while those near the plate electrodes towards the side wall. The velocity z-component reaches -0.5 m/s near the duct axis and $+0.45$ m/s at the plate electrodes.

In the measurement plane at $z = +10$ mm (Fig. 3d and e), we can see, that also in this plane the operating voltage resulted in a strong disturbance in the flow. The particle trajectories are strongly bent towards the plate electrodes and next from the plate electrodes to the ESP center. The particle flow in the z-direction is similar to that presented for measurement plane located at $z = +5$ mm (see Fig. 3c and f).

The 3D transverse flow patterns (i.e. measured in the measurement planes across the ESP) are shown in Fig. 4. They show the flow streamlines in the y–z plane and the x-component of the flow velocity. It is seen from Fig. 4a that due to the EHD forces in the y–z plane the particles flow from the ESP center (i.e. from the discharge wire electrode) towards the plate electrodes. Then, near the plate electrodes the particles turn towards the side walls, and move along them. Finally, the particles turn again towards the wire electrode. As a result, four vortices, rotating in the opposite directions, are formed in the y–z plane. Each vortex occurs in a quarter of the transverse cross section of the ESP duct. The four vortices start to form at the beginning of the discharge region, at $x = -40$ mm. Starting from this point, the vortices develop and they became strongest in the central mid-plane ($x = 0$ mm). At $x = +60$ mm the vortices weaken. In general, in the whole discharge region the vortex structures are regular and symmetric. It is seen from Fig. 4b that the velocity x-component is positive. This means that in the ESP with longitudinal wire electrode the particles move only forward and the backward flow does not exist. The velocity x-component is low near the plate electrodes, side walls and the duct axis (below 0.25 m/s). In the central part of each quarter of the transverse cross-section of the ESP duct, i.e. in the vortex center the velocity x-component reaches its highest value (about 1 m/s).

Based on the flow patterns shown in Figs. 3 and 4 one can conclude that the flow in the ESP with longitudinal wire electrode has the form of four spiral vortices moving along the flow.

3.2. The ESP with transverse wire electrode

The results of 3D PIV measurements in the ESP with transverse wire electrode are shown in Fig. 5. Similarly, as for ESP with longitudinal wire electrode, the results show the velocity fields and corresponding flow streamlines in the x–y plane as well as the z-component of the flow velocity. The flow patterns in the central measurement plane (at $z = 0$ mm) are presented in Figs. 5a–c. They show that, the primary flow is heavily disturbed by the applied voltage. Upstream, before the discharge region a regular and stable vortex is formed close to the bottom plate electrode (a symmetrically placed vortex, near the upper plate electrode is expected; however due to either a slight asymmetry of the flow at the ESP entrance or asymmetry of the discharge only a tendency to form this vortex is seen). The vortex formed at the upstream blocks the primary flow near the plate electrode and increases its velocity near the ESP axis. Near the wire electrode the flow turns towards the plate electrodes (Fig. 5a and b) and the side wall (Fig. 5c). In the downstream

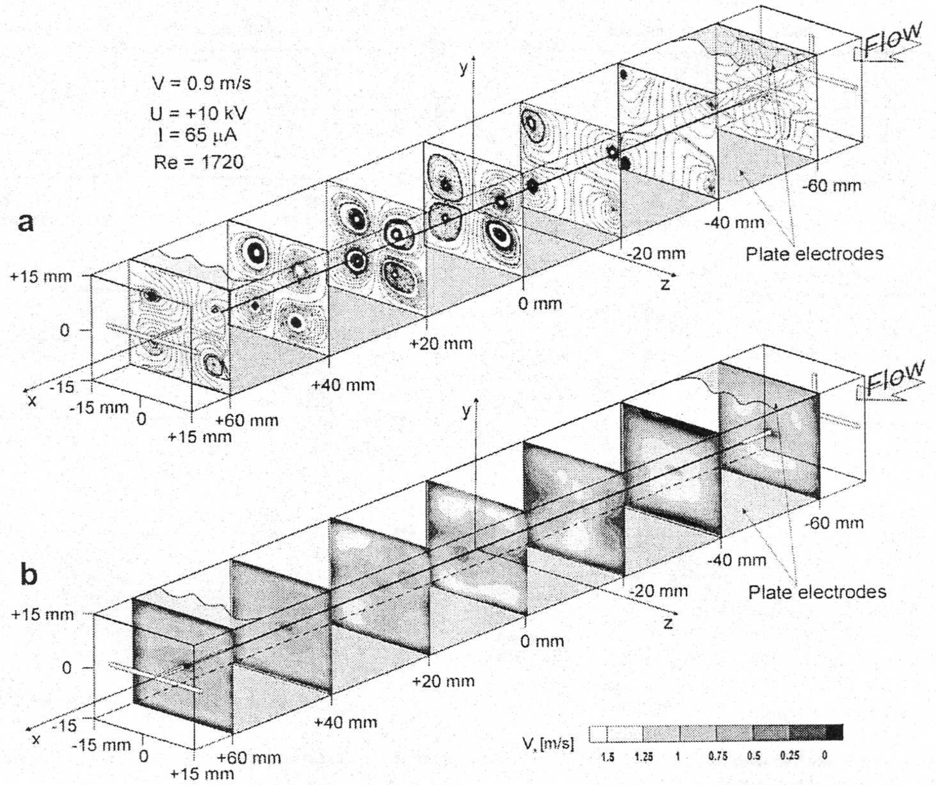

Fig. 4. Results of 3D PIV measurement in the ESP with longitudinal wire electrode in several transverse planes. The flow streamlines (a), and the velocity x-component (b).

region a backward stream at around $x = +20$ mm ÷ +60 mm exists, with a flow velocity of about 0.3 m/s. The particle movement in z-direction (Fig. 5c) is very complicated. The velocity z-component reaches value + 0.6 m/s in the central part of the ESP duct at $x = -20$ mm ÷ +20 mm. Whereas in the downstream region the velocity z-component ranged from −0.45 m/s near the plate electrodes to +0.45 m/s in the axial part of the ESP duct. One can deduce from that, in the downstream region a pair of

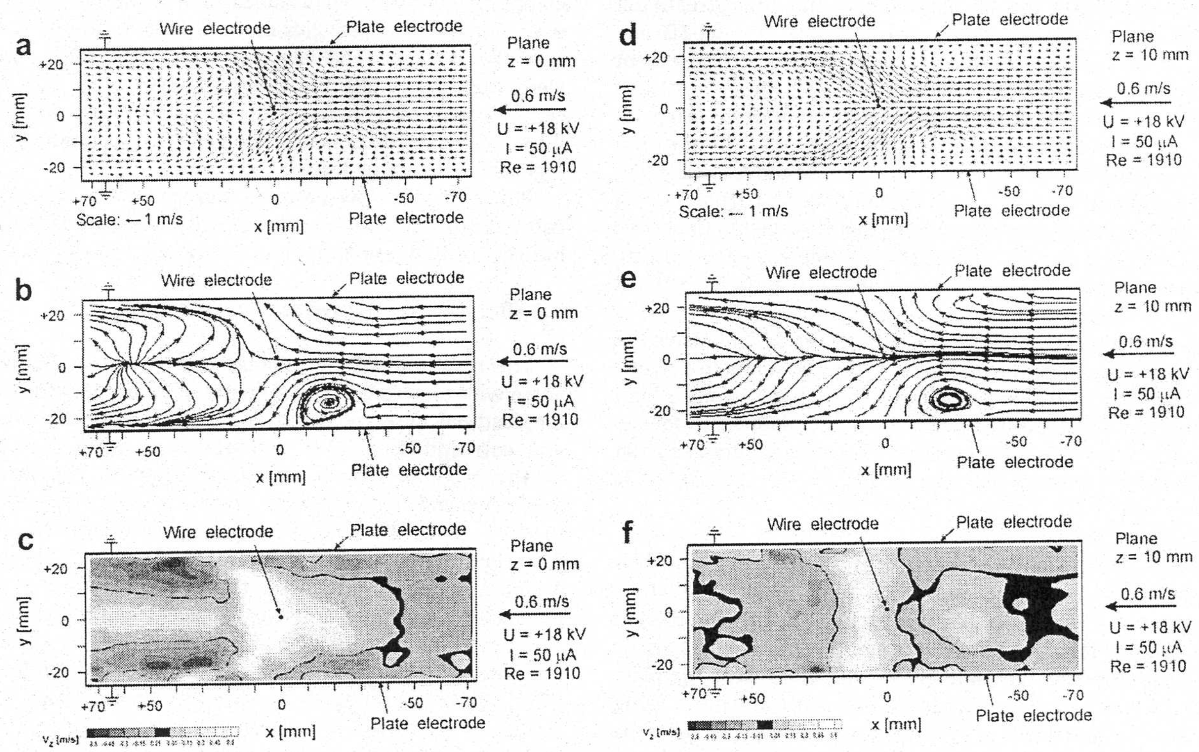

Fig. 5. Results of 3D PIV measurement in the ESP with transverse wire electrode in the plane at $z = 0$ mm and at $z = +10$ mm. The flow velocity field (a, d) and the corresponding flow streamlines (b, e), and the velocity z-component (c, f).

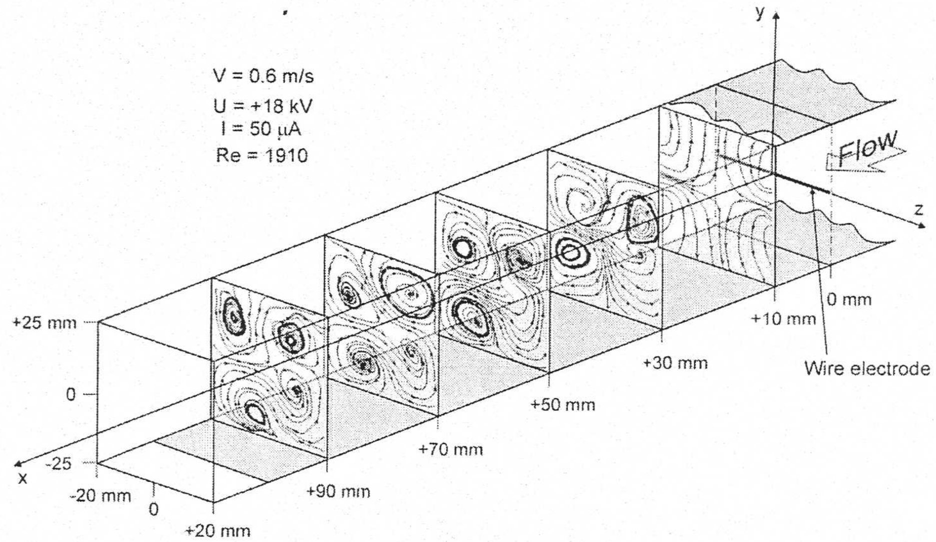

Fig. 6. The flow streamlines in the ESP with transverse wire electrode in several transverse planes.

oppositely revolving spiral vortices are formed. The revolving of these spirals is complex.

In the measurement plane at $z = +10$ mm (Fig. 5d–f), one vortex near the bottom plate electrode is formed, similarly as in the central plane $z = 0$ mm. Also similarly as in the central plane, in the plane at $z = +10$ mm the flow turns towards the plate electrodes (Fig. 5d and e) and the side wall (Fig. 5f). However, in the downstream of the flow in the plane $z = +10$ mm is less disturbed than that in the central plane (for example there is no backward flow). The vortices, shown in Fig. 5, suggest that near the plate electrodes axial flow rolls exist in the z-direction, i.e. perpendicularly to the primary flow direction. This means that the EHD forces make the flow complex.

The transverse flow streamlines in the ESP with transverse wire electrode for five measurement planes are shown in Fig. 6. It is seen from Fig. 6 that in the transverse plane at $x = 10$ mm four vortices (one in each ESP quarter) start to build up. The vortices evolve and at $x = +30$ mm they are well developed.

Comparing the transverse flow in both ESPs, with longitudinal wire electrode (Fig. 4) and with transverse wire electrode (Fig. 6) we can find that the particle flow in the transverse planes is more complicated in the ESP with transverse wire electrode.

4. Conclusions

The presented results of the PIV measurements show that the particle flow in the narrow ESP with longitudinal or transverse wire electrode exhibits a strongly 3D character due to the applied voltage and the narrow cross-section of the ESP duct.

The flow patterns in both presented ESPs (with longitudinal or transverse wire electrode) are very complicated. Several vortices were formed along and perpendicular to the ESP duct. In the ESP with longitudinal wire electrode the vortices move along the ESP and do not block the primary flow, as they do in the ESP with transverse wire electrode. This suggests that in the ESPs with the longitudinal wire electrode, the pressure drop is lower and the flow along the ESP is smoother than in the ESPs with transverse wire electrode, which is much complex. At this stage we cannot decide which ESP configuration, with longitudinal or transverse electrode is better for particle collection efficiency. An experiment is carried to elucidate this point.

References

[1] H.J. White, Industrial Electrostatic Precipitation, Wesley Publishing Company, Inc., 1963.
[2] U. Kogelschatz, W. Egli, E.A. Gerteisen, Advanced computational tools for electrostatic precipitators, ABB Rev. 4 (1999) 33–42.
[3] A. Yabe, Y. Mori, K. Hijikata, EHD study of the corona wind between wire and plate electrodes, AIAA J. 16 (1978) 340–345.
[4] T. Yamamoto, H.R. Velkoff, Electrodynamics in an electrostatic precipitator, J. Fluid Mech. 108 (1981) 1–18.
[5] J. Mizeraczyk, M. Kocik, J. Dekowski, J. Podliński, T. Ohkubo, S. Kanazawa, Visualization and particle image velocimetry measurements of electrically generated coherent structures in an electrostatic precipitator model, Inst. Phys. Conf. Series 178 (2003) 167–173.
[6] J. Podliński, A. Niewulis, J. Mizeraczyk, A. Mizuno, 3D PIV measurements of the ehd flow patterns in a narrow electrostatic precipitator with wire-plate or wire-flocking electrodes, Czech. J. Phys. 56 (Suppl. B) (2006) 1009–1016.
[7] P. Atten, H.L. Pang, J.-L. Reboud, J. Podlinski, J. Mizeraczyk, Turbulence generation by charged fine particles in electrostatic precipitators, ESA 2007 Annual Meeting, Purdue University, West Lafayette, Indiana, USA, 2007, pp. 259–270.
[8] P. Atten, F.M.J. McCluskey, A.C. Lahjomri, The electrohydrodynamic origin of turbulence in electrostatic precipitators, IEEE Trans. Ind. Appl. 23 (1987) 705–711.
[9] T. Yamamoto, Effects of turbulence and electrohydrodynamics on the performance of electrostatic precipitators, J. Electrostat. 22 (1989) 11–22.
[10] A. Aly, B.J. Sung, S.H. Lee, A. Mizuno, The effect of different configurations of collecting electrodes on the flow visualization inside a wire-plate electrostatic precipitator (ESP) in the collecting electrodes, Annual Meeting of the Institute of Electrostatics, Japan, 2005.
[11] M. Raffel, Ch.E. Willert, J. Kompenhans, Particle Image Velocimetry, A Practical Guide, Springer-Verlag, Berlin Heidelberg, 1998.